NBD-Cholesterol Probes to Track Cholesterol Distribution in Model Membranes

Carter Ramirez, Daniel M.; Ogilvie, William W.; Johnston, Linda J.

Publisher's version / Version de l'éditeur:
https://doi.org/10.1016/j.bbamem.2009.12.005
Biochimica et Biophysica Acta, 1798, 3, pp. 558-568, 2010-12-21

Biochimica et Biophysica Acta 1798 (2010) 558–568

Contents lists available at ScienceDirect

Biochimica et Biophysica Acta

journal homepage: www.elsevier.com/locate/bbamem

NBD-cholesterol probes to track cholesterol distribution in model membranes

Daniel M. Carter Ramirez [a,b], William W. Ogilvie [b], Linda J. Johnston [a,*]

[a] Steacie Institute for Molecular Sciences, National Research Council Canada, Ottawa, ON, Canada K1A 0R6
[b] Department of Chemistry, University of Ottawa, Ottawa, ON, Canada K1N 6N5

ARTICLE INFO

Article history:
Received 10 September 2009
Received in revised form 17 November 2009
Accepted 8 December 2009
Available online 21 December 2009

Keywords:
Cholesterol
Atomic force microscopy
Supported lipid bilayer
Fluorescence
Ceramide

ABSTRACT

A series of cholesterol (Chol) probes with NBD and Dansyl fluorophores attached to the 3-hydroxyl position via carbamate linkers has been designed and synthesized and their ability to mimic the behavior of natural cholesterol in bilayer membranes has been examined. Fluorescence spectroscopy data indicate that the NBD-labeled lipids are located in the polar headgroup region of the bilayer with their position varying with the method of fluorophore attachment and the linker length. The partitioning of the Chol probes between liquid-ordered (L_o) and liquid-disordered (L_o) phases in supported bilayers prepared from ternary lipid mixtures of DOPC, Chol and either egg sphingomyelin or DPPC was examined by fluorescence microscopy. The carbamate-linked NBD-Chols show a stronger preference for partitioning into L_o domains than does a structurally similar probe with an ester linkage, indicating the importance of careful optimization of probe and linker to provide the best Chol mimic. Comparison of the partitioning of NBD probes to literature data for native Chol indicates that the probes reproduce well the modest enrichment of Chol in L_o domains as well as the ceramide-induced displacement of Chol. One NBD probe was used to follow the dynamic redistribution of Chol in phase separated membranes in response to *in situ* ceramide generation. This provides the first direct optical visualization of Chol redistribution during enzymatic ceramide generation and allows the assignment of new bilayer regions that exclude dye and have high lateral adhesion to ceramide-rich regions.

1. Introduction

The raft hypothesis postulates that cellular membranes contain discrete regions enriched in sphingomyelin (SM) and cholesterol (Chol) [1,2]. These domains, termed lipid rafts, are thought to exist in a liquid-ordered (L_o) phase; as such they have a different composition from the remainder of the lipid bilayer, which is thought to be in a fluid or liquid-disordered (L_d) phase. Lipid rafts are implicated in processes involving membrane protein compartmentalization and lipid sorting such as cell signaling, membrane trafficking and viral infection [3]. It has been postulated that the enzymatic generation of ceramide promotes coalescence of small raft domains to give larger platforms, providing a mechanism for organizing signaling molecules to facilitate and amplify signaling [4,5]. Ceramide is a small hydrophobic sphingolipid that is generated in vivo by sphingomyelinase (SMase) mediated hydrolysis of SM [4,5]. The role of ceramide in cell signaling is well documented and its involvement in apoptosis, differentiation and internalization of viruses and bacteria has been extensively studied [6,7]. Ceramide also has a pronounced effect on membrane properties, forming gel phase, ceramide-rich domains in both cells and model membranes [5,6,8].

The inherent difficulties in studying small, dynamic membrane domains in cells have inspired many studies of the partitioning of lipids and proteins between ordered and disordered phases in model membranes [1,9–11]. This approach has provided valuable information on the factors that lead to membrane compartmentalization and the preference of various biomolecules for specific membrane environments. For example, a variety of studies have shown that direct incorporation of ceramide in ternary lipid mixtures with coexisting liquid phases leads to gel phase ceramide-rich domains and to the expulsion of Chol from liquid-ordered phases [12–22]. Although the consequences of direct ceramide incorporation are reasonably well-understood, enzymatic ceramide generation is more complex, even in model membranes [12,14,21,23–27]. Recently, we have used a combination of atomic force microscopy (AFM) and fluorescence to demonstrate that enzymatic generation of ceramide leads to significant membrane restructuring of phase separated lipid bilayers with coexisting L_o and L_d phases [24,25]. These changes include formation of ceramide-enriched regions in the original L_o domains and the disappearance of some domains with the concomitant formation of new membrane regions that exclude dye and have different thickness and higher lateral adhesion than the initial L_o and L_d phases. The multi-modal imaging approach allowed us to probe changes on the nanometer scale using AFM and to follow the dynamics of the larger scale bilayer restructuring using fluorescence, providing significant insight into this complex process. Nevertheless, it was not possible to draw definitive conclusions on the composition

* Corresponding author.
E-mail address: Linda.Johnston@nrc-cnrc.gc.ca (L.J. Johnston).

0005-2736/$ – see front matter
doi:10.1016/j.bbamem.2009.12.005

(ceramide-rich vs Chol-rich) of new regions of high lateral adhesion that were generated [25]. Although we considered the possibility of probing Chol distribution with an antibody, our previous work had shown that labeling L_o domains with GM1 cholera toxin significantly reduced enzyme-induced membrane restructuring. Thus, we employed an alternate approach using a dye-labeled Chol to evaluate Chol redistribution during enzymatic reaction.

Fluorescence microscopy has been widely used to visualize L_o–L_d phase separation for ternary lipid mixtures that model some aspects of membrane raft behavior but there are few probes that can selectively label ordered Chol and sphingolipid-rich domains [28,29]. As demonstrated recently by Feigenson and Webb, most fluorescent lipid analogs partition strongly into the L_d phase based on fluorescence microscopy studies in giant unilamellar vesicles (GUVs) [28]. The membrane partitioning behavior of a number of fluorescent Chol derivatives has been examined with three main strategies employed for fluorophore incorporation [30]. First, naturally fluorescent sterols such as cholestatrienol have been shown to mimic Chol in lipid trafficking and in sterol-rich domains in lipid bilayers [31,32]. This approach avoids modification of the hydroxyl group and the alkyl chain, thus minimizing disruption of Chol packing in L_o phases, but has significant limitations due to rapid photobleaching and the requirement for UV excitation [28,33]. Second, Chol analogs with dyes such as NBD attached to the aliphatic side chain have been shown to partition into disordered phases and do not duplicate the membrane condensation effect of native Chol [28,29,32]. By contrast, attachment of a hydrophobic fluorophore to the aliphatic side chain is more successful since a Bodipy-Chol analog was shown to condense phosphatidylcholine (PC) monolayers and support the formation of a SM Chol ordered phase [34]. However, fluorescence microscopy of supported bilayers of DOPC/SM/Chol mixtures indicates that this probe is very sensitive to the bilayer composition, localizing in either ordered (brain SM) or disordered (C_{16}-SM) phases or showing no contrast (C_{18}-SM) [35]. Direct measurements of partition coefficients by fluorescence correlation spectroscopy confirm these qualitative conclusions from fluorescence intensity ratios, with K_p (L_o/L_d) of 1.9 and 0.8 for DOPC/egg SM/Chol GUVs and DOPC/C_{18}-SM/Chol supported bilayers [13,36]. Third, several studies indicate variable results for hydroxyl-labeled Chols. For example, replacement of the 3-hydroxyl with a doxyl spin label did not significantly modify the behavior compared to natural Chol based on NMR order parameters [32], whereas a Bodipy-labeled Chol ester partitioned strongly into liquid-disordered domains [37]. The above results demonstrate that the choice and method of attachment of the dye require careful adjustment to design a fluorescent analog that reproduces the behavior of natural Chol.

We have synthesized 4 novel fluorescent Chols (Fig. 1, **1–4**) that are labeled with fluorophores at the 3β-OH position, characterized their fluorescence behavior in vesicles and examined their suitability for visualization of phase separation in supported bilayers with coexisting L_o and L_d phases. A combination of fluorescence and AFM shows that the various Chol analogs have modest preferences for either L_o or L_d phases, depending on the lipid composition, the fluorophore and the length of the linker. One derivative has been used to probe Chol displacement by direct ceramide incorporation in bilayers containing SM. The same probe was employed to follow the dynamics of membrane reorganization during enzymatic generation of ceramide, providing the first direct visualization of enzyme-mediated Chol redistribution, as well as information on the bilayer composition after *in situ* ceramide generation.

2. Materials and methods

2.1. Materials

Dioleolylphosphatidylcholine (DOPC), dipalmitoylphosphatidylcholine (DPPC), chicken egg sphingomyelin (ESM), $C_{16:0}$ ceramide (Cer), cholesterol (Chol), 1,2-dipalmitoyl-*sn*-glycero-3-phospho ethanolamine-N-(7-nitro-2-1,3-benzoxadiazol-4-yl) (ammonium salt) (N-NBD-DHPE), and 5-cholesten-3β-ol 6-[(7-nitro-2-1,3-benzoxadiazol-4-yl)amino]caproate (NBD-6 Chol, **5**) were purchased from Avanti Polar Lipids (Alabaster, AL) and were used as received. Texas Red 1,2-dihexadecanoyl-*sn*-glycero-3-phosphoethanolamine, triethylammonium salt (TR-DHPE) was obtained from Invitrogen (Eugene, OR). Chol analogs **1–4** were synthesized from Chol and NBD-alkylendiamines as described in the Supplementary material. Sphingomyelinase (SMase) isolated from *Staphylococcus aureus* was obtained from Sigma-Aldrich. All aqueous solutions were prepared using 18.3 MΩcm Milli-Q water. SMase buffer: 125 mM NaCl, 10 mM $CaCl_2$, 2 mM $MgCl_2$, 10 mM HEPES, pH 7.4.

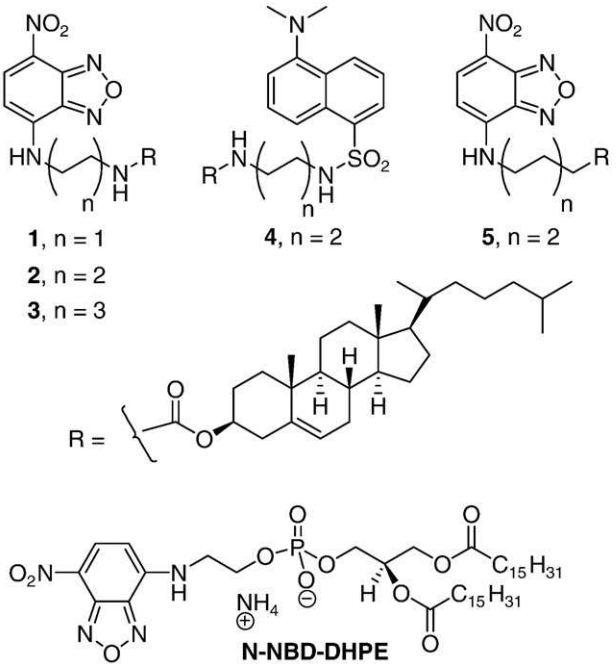

Fig. 1. Structures of the labeled Chols and the N-NBD-DHPE standard used in this study.

2.2. Preparation of bilayers

Small unilamellar vesicles were prepared with minor adjustments to a previously described protocol [14]. Briefly, chloroform solutions of phospholipids and dye-labeled lipids were mixed in the appropriate ratios and the lipid films obtained after evaporating the solvent were hydrated in water. The samples were then sonicated in a bath sonicator to clarity to form SUVs with a final lipid concentration of 0.5 mg/mL. All vesicle solutions were sonicated at temperatures above the T_m of the constituent lipids and were used immediately or stored at 4 °C for up to 1 week prior to use.

Planar supported bilayers were formed on mica via vesicle fusion. Vesicle solution (60 μl) and 750 μl $CaCl_2$ (15 mM) were added to freshly cleaved mica (15–25 μm thick for fluorescence imaging) clamped in a liquid cell. After incubation at 45 °C for 60 min, bilayers were gradually cooled to RT over a period of 2 h, and then gently washed with Milli-Q water to remove unattached vesicles before imaging. The presence of occasional defects allowed us to measure the bilayer thickness, confirming the presence of a single bilayer.

2.3. Spectroscopic measurements

Absorption spectra were measured with a Cary 5000 UV–vis-NIR spectrophotometer at 22 °C, using a 1-cm-path length quartz cuvette. Absorption spectra for NBD-labeled Chols **1–3** and **5**, and N-NBD-

DHPE were measured in water at 0.5 mol% dye to total lipid in vesicles, with the total lipid concentration at 1.3×10^{-3} M. The spectra of vesicle solutions containing dye-labeled lipids were corrected for scattering using a vesicle solution of the same lipid composition in the absence of dye. Emission spectra were recorded at 22 °C using a Horiba Jobin Yvon FL3-21 2tau spectrofluorometer with slit widths of 1 nm. Fluorescence quantum yields Φ were obtained with reference to N-NBD-DHPE in vesicles of egg yolk PC ($\Phi=0.16$ [38]) at an excitation wavelength of 470 nm and absorbance <0.2.

2.4. Fluorescence microscopy

Fluorescence images of most bilayers were measured in total internal reflection fluorescence (TIRF) mode on an Olympus 1X81 microscope equipped with a high resolution CCD camera (CoolSNAP, Photometrics, US) and a 60×/1.45 NA Plan Apochromat objective. The NBD-labeled Chols were excited at 488 nm and emission collected at 530 (±20) nm. Dansyl-Chol images were obtained using an arc lamp and a UV excitation/visible emission filter set (Semrock) in epifluorescence mode. For SMase treatment, the bilayers were washed with SMase buffer and imaged. The effect of enzyme on the bilayer was followed in time by imaging the same area before and after addition of buffered enzyme solution at room temperature. Control experiments indicated that irradiation of bilayers containing NBD-Chol **2** for similar time periods to those used for the SMase treatments led to no changes in bilayer morphology, although significant photobleaching of the dye was observed. The use of TIRF microscopy is an advantage, even for thin bilayer samples, because background fluorescence from residual vesicles in the solution does not contribute to the bilayer signals. This is particularly useful for studies of SMase-treated bilayers since enzyme activity frequently leads to release of fluorescent vesicles into the solution.

For the fluorescence intensity analysis, the intensity counts of adjacent domain and fluid-phase regions were obtained using ImagePro software. A background fluorescence count was obtained by either completely bleaching an area immediately adjacent to the area-of-interest or by using a bilayer defect in the region of interest. Care was taken to ensure that background, domain and fluid phase intensities were measured within a small area (2–4 μm) with uniform excitation intensity to minimize effects due to variation in excitation intensity across the field of view. Several different areas were imaged for each sample. The relative intensities of adjacent L_d fluid-phase and L_o domains were taken from intensity cross sections of the area-of-interest. These values were then corrected for background fluorescence to give an L_d/L_o intensity ratio (I_{Lo}/I_{Ld}). A minimum of ten corrected I_{Lo}/I_{Ld} values were collected per region (approximately 100 μm^2), and a number of different samples were measured for each analog to check for reproducibility.

2.5. Quantification of bilayer standards

Relative quantum yield measurements for supported bilayers were measured using a recently reported procedure for quantifying fluorescence microscopy data using supported bilayer standards [39]. First, plots of fluorescence intensity vs [probe **2**] in DOPC bilayers were measured (in epifluorescence mode on an IX81 inverted optical microscope) and shown to be linear between 0.1 and 1.0 mol% dye (Fig. S1). Then fluorescence intensities for single phase bilayers of DOPC, DOPC/Chol, DOPC/ESM and DOPC/DPPC (all 2:1 molar ratios) containing 0.5 mol% **2** were measured under matched conditions. To account for variations in spectral properties of the probe in different lipid environments the intensity data was corrected using a scaling factor measured on the same microscope. This was accomplished by measuring the fluorescence intensity of vesicle solutions used to prepare the supported bilayers by focusing the excitation laser deep into the sample and verifying that the intensity measured did not vary with small changes in the focus. The ratio of corrected intensities for DOPC/Chol and DPPC (or ESM)/Chol bilayers provides an estimate of the relative quantum yields for probe **2** in L_o/L_d phases.

2.6. Correlated fluorescence-atomic force microscopy

Correlated images were recorded using a JPK NanoWizard®II BioAFM (JPK Instruments, Berlin, Germany) integrated with an Olympus IX81 inverted optical microscope. AFM was performed in contact mode and images were captured using DNP-S (Veeco, CA) AFM cantilever/tips with spring constants of 0.15–0.32 N/m. Images were recorded in both topographic and lateral deflection modes. The contrast in lateral deflection scans depends strongly on the normal force applied to the sample and the scan speed. Epifluorescence images were obtained using lamp excitation with a 100× oil immersion objective (Olympus), FITC WF filter set (Chroma Technology) and a high resolution CCD camera (CoolSNAP, Photometrics).

Solid-supported bilayers of the desired composition were prepared and AFM and fluorescence images of the same sample area were recorded sequentially, after locating a suitable sample region. Fluorescence images had acquisition times of <3 s, much shorter than the ~10 min required to obtain the AFM images. Typically fluorescence images were recorded both before and after AFM images of the same area to verify that the membrane morphology had not changed dramatically during the time required for AFM imaging. For SMase treatment the bilayer was imaged in water (using both techniques) prior to replacing the water with a known volume of buffered enzyme solution; this was followed by incubating the sample at room temperature for 10–20 min while following its evolution by fluorescence microscopy. The sample was then rinsed extensively with water and re-imaged by both AFM and fluorescence.

3. Results

3.1. Design and synthesis of cholesterol analogs

Based on the advantages and limitations of the fluorescent sterols that have been examined previously, we chose to synthesize Chol probes with dyes conjugated at the 3-hydroxyl position. This choice was based on the observation that Chols with polar fluorophores attached to the aliphatic tail show a preference for labeling disordered phases [28], while partitioning of the tail-labeled Bodipy-Chol is very sensitive to the membrane composition, specifically the chain length and heterogeneity of the SM component [13,35,36]. We selected the small, polar NBD fluorophore, reasoning that the failure of the Bodipy-Chol esters to partition into ordered domains [37] was due to insertion of the hydrophobic Bodipy moiety into the membrane, disrupting lipid packing. NBD is an environment sensitive dye with fluorescence quantum yields that vary with solvent polarity, and has been widely used as a probe in cells and model membranes [38,40]. The NBD fluorophore was attached via a carbamate group, as used previously to attach a Dansyl chromophore to the C-6 position [41]; the carbamate group is resistant to hydrolysis and retains some of the hydrogen bonding capability of the free hydroxyl group. Diamine linkers with 2, 4 and 6 carbons were used to determine the optimal linker length to minimize disruption of the polar head group packing by the fluorophore. NBD-Chols **1–3** have intramolecular distances between C-3 of the sterol and C-4 of the fluorophore ranging from 8.5 to 13.5 Å, based on calculations for the lowest energy, anti-staggered linker conformation. We also synthesized one analog with a Dansyl fluorophore, which is similar in size to NBD but less hydrophilic. Synthesis and characterization of probes **1–4** are described in the Supplementary material. The structures for dye-labeled Chols (**1–4**), a commercially available NBD-Chol ester with a 6-carbon linker (**5**) that was used for comparison and the N-NBD-DHPE standard are shown in Fig. 1.

3.2. Fluorescence spectroscopy

Absorption and fluorescence spectra were measured for NBD-Chols **1**–**3** and **5** and N-NBD-DHPE in aqueous vesicle solutions of 2:1 DOPC/Chol, 2:1 DPPC/Chol, and 2:1 ESM/Chol. These mixtures were selected to approximate the composition of the L_d and L_o phases in the domain-forming bilayers used for fluorescence microscopy; representative data for several probes in DOPC were also measured. The absorption spectra for all four probes were similar with maxima at 335 and 470 (±5) nm, corresponding to the π, π* and charge transfer bands, respectively. The maximum of the fluorescence emission spectra varied by ~10 nm for the various probe/lipid combinations, ranging from 527 to 537 nm, Supplementary material, Table S1. The emission maxima are similar to literature values of 541 and 535 nm for N-NBD-DHPE and several acyl chain labeled phospholipids in fluid vesicles [38,40]. They are significantly blue-shifted from the 566 nm emission maximum reported for n-propylamino-NBD in water, reflecting the less polar environment of the lipid bilayer [42].

Fluorescence quantum yields, Φ, were determined in the same lipid vesicles (Table S2) using N-NBD-DHPE in DOPC vesicles (Φ of 0.16 at 2.0 mol% dye in egg PC) as a standard [38]. Φ values for the NBD-labeled lipids ranged from 0.12 to 0.26 for the different lipid compositions, indicating relatively modest changes in the polarity experienced by the NBD fluorophore as a function of either probe structure or lipid composition. The effect of probe concentration in ESM/Chol was examined for **2** (Table S2); the quantum yield decreased by less than a factor of two over a probe concentration range of 0.1 to 1 mol%.

3.3. Partitioning of dye-labeled cholesterols in ternary lipid mixtures

Lipid mixtures of DOPC, DPPC or ESM, and Chol in a 2:2:1 mol ratio and containing 0.5 mol% of the dye-labeled lipids were used as a starting point to study the partitioning behavior of the new Chol analogs. Supported lipid bilayers of these mixtures display coexisting L_o/L_d phases and afford L_o domains large enough to visualize using fluorescence microscopy, as reported in previous studies [14,25,43]. Representative images for DOPC/ESM/Chol and DOPC/DPPC/Chol bilayers containing 0.5 mol% probe **2** are shown in Fig. 2A, B. The bilayer for the ESM mixture has many small dye-excluded regions that correspond well to the dark domains observed for this mixture using Texas Red-DHPE to visualize phase separation in our earlier work [14,25]. The contrast between domains and fluid phase is much lower than that observed for Texas Red-DHPE which has approximately 3-fold higher intensity in the fluid phase than in the domains. The image in Fig. 2A provides qualitative evidence for a modest preference of the labeled Chol for the fluid phase. By contrast, the image in Fig. 2B for the DOPC/DPPC/Chol bilayer shows small bright domains, indicating that probe **2** preferentially stains the ordered domains; AFM was used to verify that the bright regions corresponded to higher liquid-ordered domains.

Since the two raft mixtures showed different partitioning behavior for probe **2**, we examined several additional compositions within the L_d/L_o co-existence region for DOPC/ESM/Chol membranes (Fig. 2) [43,44]. The bilayer morphology changed as the lipid composition was varied and AFM was used to verify the assignment of dye-excluded areas to either fluid or ordered regions. Representative data for correlated fluorescence and AFM imaging of a 7:9:4 DOPC/ESM/Chol bilayer are shown in Fig. 3. The darker regions in the optical image (Fig. 3A) correspond to raised domains and higher frictional contrast in the AFM height and lateral deflection scans, respectively (Fig. 3B, C), consistent with their assignment to areas of L_o phase. Similarly, the areas of stronger fluorescence match the phase with lower height and lower frictional contrast observed by AFM, and are identified as the fluid or L_d phase (Fig. 3D). Comparison of AFM and fluorescence images for the other compositions indicates that probe **2** partitions more strongly into the L_d phase in all but one of the ESM mixtures (see representative fluorescence images in Fig. 2C–F). The exception is the bilayer with the highest fraction of ESM (3:5:2 DOPC/ESM/Chol, 50% ESM, fluorescence in Fig. 2C, AFM not shown) where the ordered phase has the stronger fluorescence; this composition gave interconnected domains, making it difficult to distinguish L_o and L_d phases based solely on the fluorescence images. The AFM and fluorescence images for mixtures with variable ESM ratios indicate that domains of the higher ordered phase become less round and increasingly irregular in shape and cover a larger fraction of the surface area as the fraction of ESM increases. The 1:1:1 bilayers typically exhibited smooth, round domains (Fig. 2F) that were consistently larger than those for the other ESM mixtures.

For comparison to literature data [45], DOPC/brain SM/Chol bilayers (3:2:1 and 4:2:1) containing 0.5 mol% probe **2** were imaged by fluorescence microscopy and AFM. These mixtures gave higher liquid-ordered domains (as visualized by AFM) that were slightly darker than the surrounding membrane in fluorescence images; representative images are shown in Fig. S2. Thus, both egg and brain SM have qualitatively similar partitioning behavior for NBD-Chol **2**.

The ratios of intensities (I_{Lo}/I_{Ld}) for L_o and L_d phases in bilayers of various ternary lipid mixtures with 0.5 mol% of probes **1–5** were measured for multiple bilayers for each probe/lipid composition (Table 1). The differences between probes and for different lipid compositions are modest, with a slight preference for localization in the L_d phase in most cases. Intensity ratios are one of the most important factors for assessing the utility of probes for labeling specific membrane domains for microscopy experiments. However, the intensity ratios reflect changes in both probe concentration and probe brightness and thus provide only qualitative information on the partitioning of probes between lipid environments. For example, a probe may show stronger fluorescence in one phase due to changes in its photophysical behavior, rather than a higher concentration. Changes in probe brightness are caused by variation in quantum yields, concentration-dependent self-quenching or excitation efficiency (due to different molecular orientations) as a function of lipid environment [28]. Although many investigations of probe partitioning are based solely on a comparison of fluorescence intensities, others report directly measured partition coefficients, making a quantitative comparison between the two types of measurements problematic.

Differences in probe brightness between L_o and L_d phases for **2** were measured in order to estimate partition coefficients from the fluorescence intensity data for this probe in supported bilayers [39]. First, plots of fluorescence intensity as a function of [**2**] in DOPC bilayers were linear between 0 and 1% (Fig. S1), demonstrating that self-quenching does not occur at the dye concentration (0.5%) used for the phase separated bilayers. Although self-quenching has been reported for NBD-labeled lipids in vesicles, it occurs over a higher range of concentrations (eg, between 3 and 9% for C12-NBD-PC) [46]. Second, the relative quantum yields for probe **2** in different lipid environments were estimated from fluorescence intensity measurements for single phase DOPC, DOPC/Chol, DPPC/Chol and ESM/Chol bilayers under matched conditions, as outlined in the Materials and Methods. PC or SM/Chol mixtures with 2:1 molar ratios were used, providing an upper limit for the fraction of Chol in the L_o and L_d phases. The intensity ratios provide an estimate for the ratio of quantum yields for L_o vs L_d phases of 0.72 and 0.76 for ESM and DPPC mixtures, respectively. The ratio of quantum yields measured for vesicles of the same composition in solution gives similar results (0.73 and 0.79 for ESM and DPPC mixtures, respectively). This validates the approach based on quantification of intensities from supported lipid bilayers [39] and indicates either that the solid support does not affect the probe brightness or that the effect of the support is similar for both ordered and disordered phases. The quantum yield ratios for probe **2** were then used to estimate K_p from the (I_{Lo}/I_{Ld}) data for phase separated bilayers of ternary lipid mixtures (Table 1). Note that this

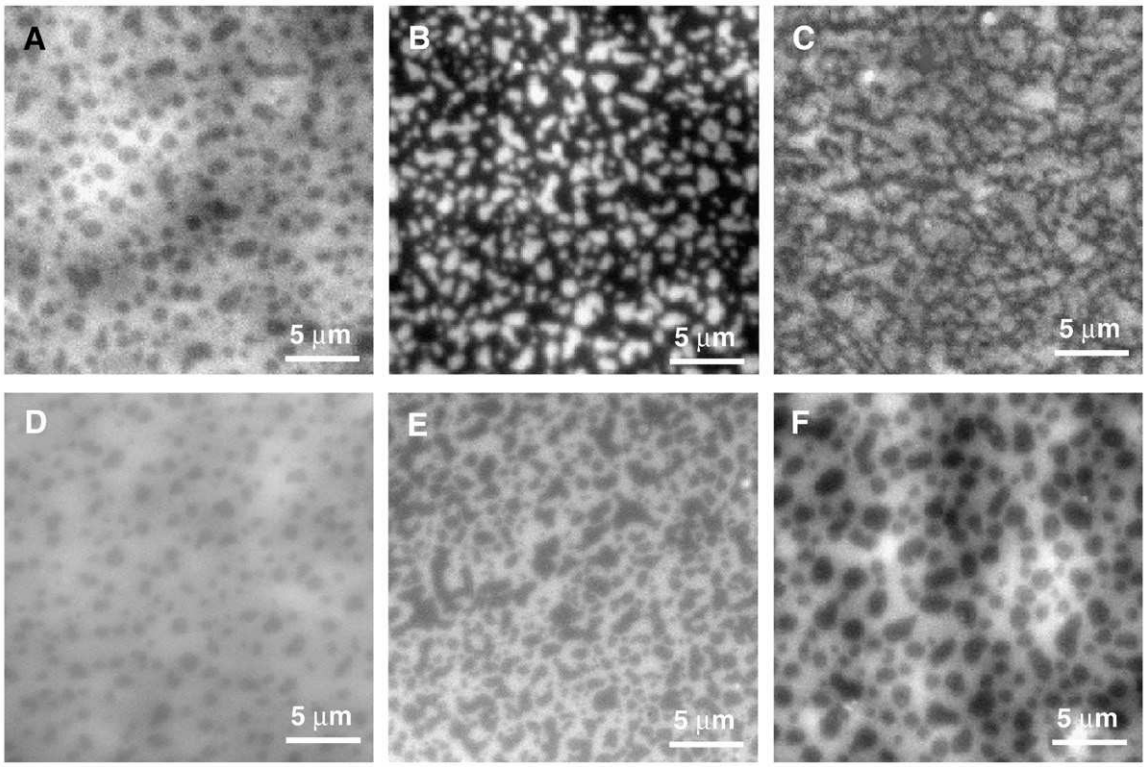

Fig. 2. Fluorescence images (TIRF) illustrating the partitioning of NBD-Chol **2** (0.5 mol%) between liquid-ordered and liquid-disordered phases in supported lipid bilayers prepared from ternary lipid mixtures: (A) DOPC/ESM/Chol 2:2:1; (B) DOPC:DPPC:Chol 2:2:1; (C) DOPC/ESM/Chol 3:5:2; (D) DOPC/ESM/Chol 5:3:2; (E) DOPC/ESM/Chol 7:9:4; (F) DOPC/ESM/Chol 1:1:1.

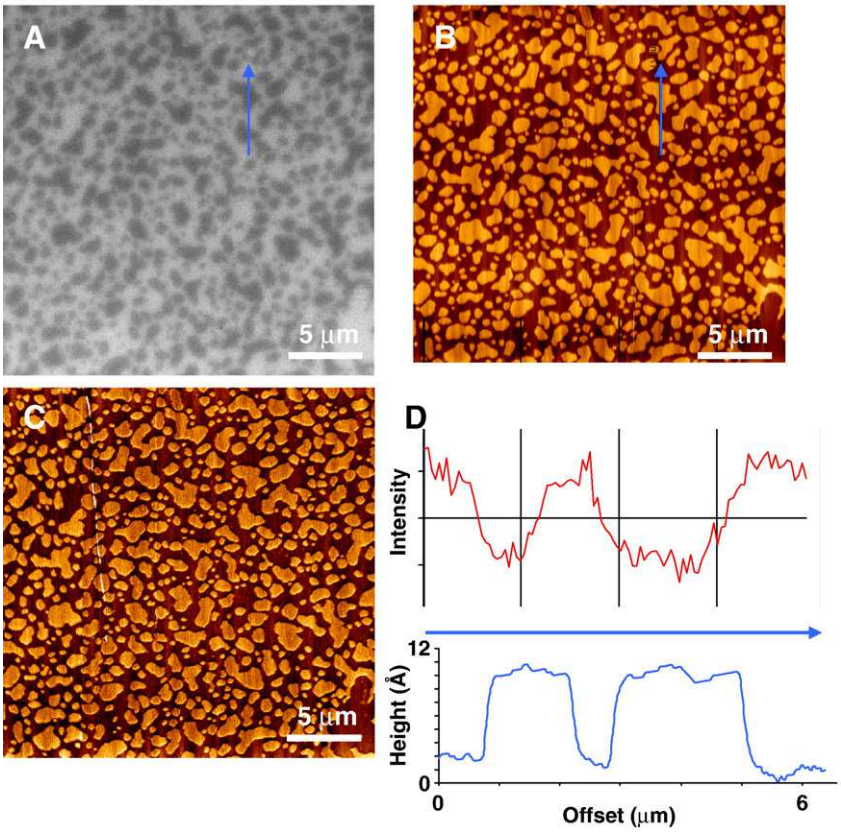

Fig. 3. Correlated fluorescence and AFM images for a DOPC/ESM/Chol (7:9:4) supported lipid bilayer containing 0.5 mol% NBD-Chol **2**: (A) epifluorescence image; (B, C) height and lateral deflection AFM images, respectively; (D) intensity and height cross sections for the lines indicated in A and B. The cross sections indicate that the raised L_o domains observed by AFM are ~0.8 nm higher than the surrounding L_d phase and correspond to the dark, dye-excluded regions in the fluorescence image.

Table 1
Ratio of fluorescence (I_{Lo}/I_{Ld}) intensities and partition coefficients (K_p) for liquid-ordered/liquid-disordered phases for Chol analogs **1–5** in bilayers with various lipid compositions. Data from TIRF microscopy, except for probe 4 and Cer and brain SM mixtures, which were measured by epifluorescence.

Lipid composition[a]	Dye	I_{Lo}/I_{Ld}	K_p[b]
DOPC/DPPC/Chol			
2:2:1	1	0.77 ± 0.04	0.65
2:2:1	2	1.37 ± 0.08	1.0
2:2:1	3	1.26 ± 0.07	1.8
2:2:1	4	0.55 ± 0.03	
2:2:1	5	0.69 ± 0.04	0.4
DOPC/ESM/Chol			
2:2:1	1	0.83 ± 0.04	1.1
2:2:1	2	0.94 ± 0.02	0.7
2:2:1	3	0.90 ± 0.02	1.0
2:2:1	4	0.49 ± 0.04	
2:2:1	5	0.73 ± 0.05	0.4
3:5:2	1	0.79 ± 0.04	1.0
3:5:2	2	1.11 ± 0.02	0.8
3:5:2	3	0.79 ± 0.03	0.8
5:3:2	2	0.89 ± 0.02	0.6
7:9:4	2	0.89 ± 0.04	0.6
1:1:1	2	0.86 ± 0.04	0.6
DOPC/ESM/Chol/Cer			
7:7:4:2	2	0.53 ± 0.05[c]	
DOPC/brain SM/Chol			
3:2:1	2	0.88 ± 0.05	
4:2:1	2	0.90 ± 0.04	

[a] Molar ratios.
[b] K_p for probe **2** was estimated using relative quantum yields from supported bilayer experiments; for other probes quantum yield ratios for vesicle solutions were used.
[c] I_{gel}/I_{Ld} for ceramide-enriched domains is 0.27 ± 0.06.

approach assumes that self-quenching is negligible (consistent with the linear dependence of intensity on probe concentration) but does not account for changes in excitation due to different orientations in the supported bilayer [39]. Based on the similarity in quantum yield ratios for probe **2** in L_o and L_d phases measured for supported bilayers and vesicles, K_p values for the other NBD-Chol probes were obtained using the quantum yield data for vesicles.

3.4. Partitioning of NBD-cholesterol **2** in ceramide-containing lipid bilayers

Bilayers prepared from vesicle solutions of DOPC, ESM, Chol, and synthetic ceramide (16:0) in a 7:7:4:2 ratio containing 0.5 mol% NBD-Chol **2** were imaged by AFM and fluorescence microscopy (Fig. 4A, B). The AFM height image shows irregularly shaped domains with two distinct heights. The lower domains are ~1 nm higher than the surrounding DOPC-rich phase (Fig. 4C), consistent with the results for L_o domains in bilayers without Cer (Fig. 3). The higher areas are assigned to ceramide-rich domains, based on earlier studies that have shown that direct incorporation of ceramide leads to ceramide-enriched domains adjacent to or within the initial liquid-ordered domains for ternary lipid mixtures containing SM [12–14,24]. As described previously [25,47], the apparent height of the ceramide-rich subdomains is extremely sensitive to the force applied, varying from as much as 3–4 nm at relatively high setpoint (cross section in Fig. 4C) and decreasing to ~1 nm at lower setpoint/force.

The fluorescence image of the same region scanned by AFM shows two different intensity levels associated with the domains (Fig. 4B, C). The ceramide-enriched regions observed by AFM correspond to the darkest domains while the intermediate height L_o domains have an intensity intermediate between those of the ceramide-rich domains and the bright L_d phase. The correlated AFM and fluorescence images provide qualitative evidence that probe **2** has a lower preference for the ceramide-enriched regions than for the L_o domains (Table 1). The I_{Lo}/I_{Ld} ratio (Table 1) suggests an increased preference for probe **2** to partition into the L_d phase in the presence of ceramide, possibly reflecting a small fraction of ceramide in the L_o domains.

3.5. NBD-cholesterol **2** in sphingomyelinase-treated bilayers

Probe **2** was used to follow membrane restructuring during SMase treatment of supported bilayers prepared from 7:9:4 DOPC/ESM/Chol lipid mixtures. Prior to enzyme addition AFM shows higher L_o domains that correspond to the slightly darker areas visualized by fluorescence microscopy in a correlated imaging experiment (Fig. 3). The bilayer was treated with SMase, and fluorescence images of the same area were recorded over a period of 20 min (Fig. 5). Changes in the bilayer appeared shortly after enzyme addition, with the most dramatic restructuring events occurring on the timescale of a few minutes. Dark, dye-excluded patches formed within the first minute and grew rapidly in diameter over the first 5 min following enzyme addition (areas 1 and 2 in Fig. 5B, C). Whereas bilayers prior to enzyme addition show only two levels of fluorescence, an intensity cross section for the bilayer 5 min after enzyme addition demonstrates that the dark dye-excluded regions have considerably lower fluorescence intensity than the surrounding L_o domains, which are in turn less intense than the fluid phase (compare cross sections a and b in Fig. 5). The original domains are no longer visible in the dye-excluded patches (areas 1 and 2) that form after enzyme addition, but in other areas the original domains persist largely unchanged (area 3).

Images recorded after 10 min show the presence of bright, steadily expanding rings that surround the large dark regions (see the bright

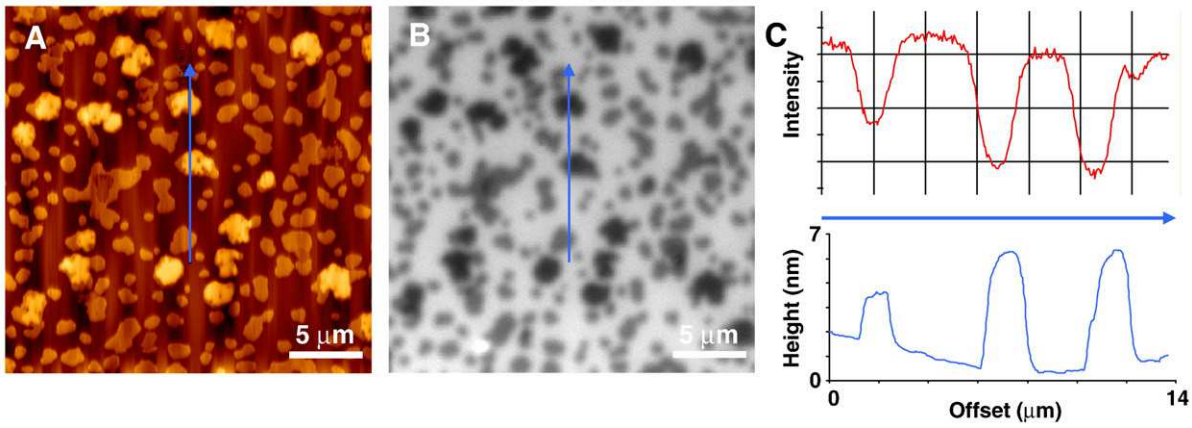

Fig. 4. Correlated AFM and fluorescence images for a DOPC/ESM/Chol/Cer (7:7:4:2) supported lipid bilayer containing 0.5 mol% NBD-Chol **2**: (A) AFM topography; (B) fluorescence image; (C) fluorescence intensity and height cross sections for the lines indicated in images A and B. The highest domains are assigned to a Cer-rich gel phase and correspond to the darkest domains in the fluorescence image, while L_o domains with intermediate height correspond to areas of intermediate intensity in the fluorescence image.

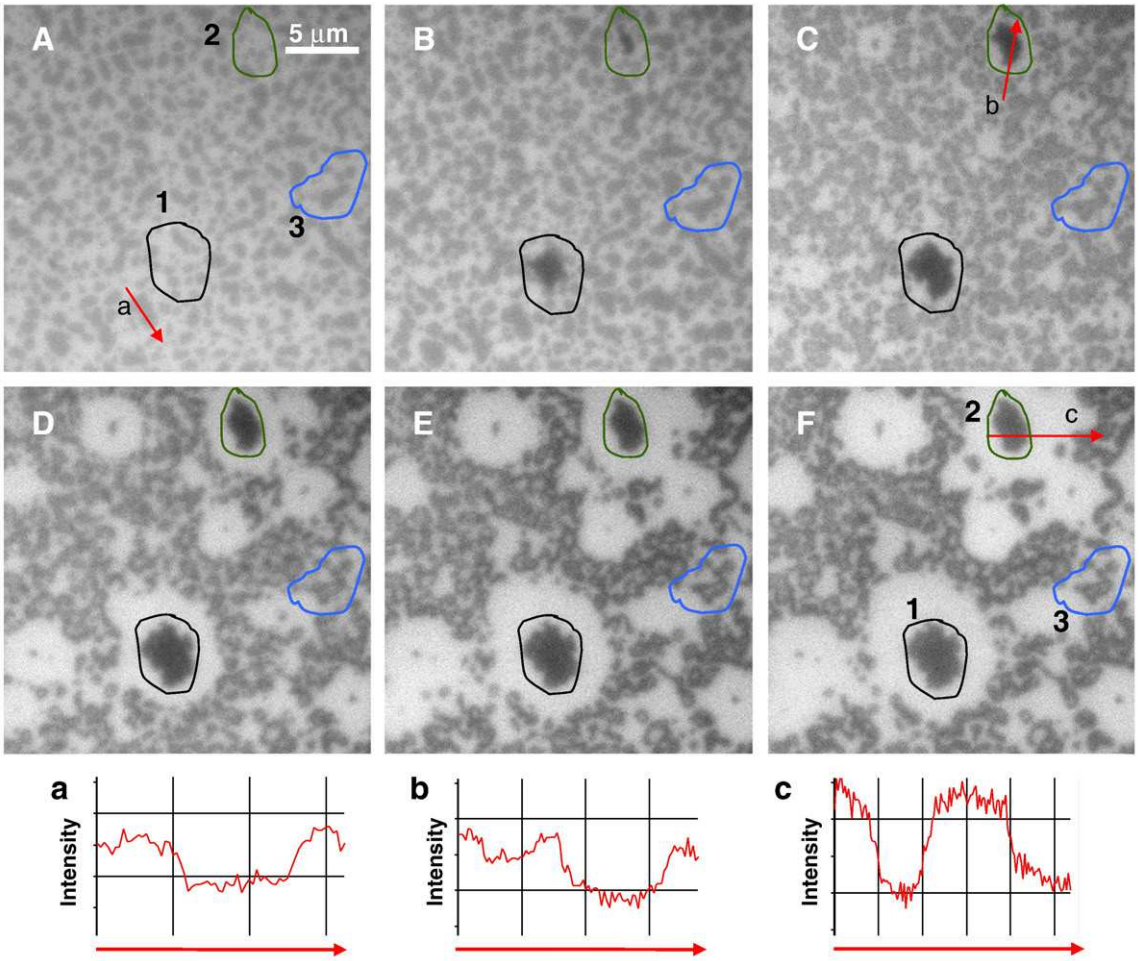

Fig. 5. Fluorescence images for a DOPC/ESM/Chol (7:9:4 with 0.5 mol% **2**) supported lipid bilayer before and during incubation with 0.33 U/ml SMase: (A) bilayer before enzyme addition; (B–F) bilayer imaged at 2.5, 5, 10, 15 and 19 min after SMase addition. Three regions of the bilayer are marked (1–3) and referred to in the text. Cross sections (a, b, c) are shown for the lines indicated in images A, C and F. Only two levels of fluorescence intensity are observed before (A, a) and at longer times after enzyme addition (F, c), while three intensity levels are evident at intermediate times (C, b).

rings around areas 1 and 2 in Fig. 5D–E). Other regions of the bilayer have a mixture of bright and dark areas that retain the outlines of the original domains. By the end of the time course, the small dark domains are of similar intensity to the large dye-excluded patches that grow in, rather than of intermediate intensity as for the image recorded at 5 min (Fig. 5F and cross section c for area 2). The dark patches and bright rings in the fluorescence images recorded during enzyme treatment for 7:9:4 DOPC/ESM/Chol bilayers are qualitatively similar to our earlier observations for bilayers prepared with different ratios of the same lipids and using Texas Red-DHPE to visualize bilayer morphology [24,25]. However, the NBD-labeled Chol probe provides additional information on changes in Chol distribution, suggesting that Chol is excluded from the dark patches that form during enzyme action, as well as from the domains.

To confirm the above hypothesis, the bilayer was washed to inactivate/remove enzyme and correlated AFM and fluorescence images were recorded (Fig. 6). Although a different area is imaged after washing, the fluorescence image (Fig. 6A) has similar features to those in Fig. 5F; cross sections (Fig. 6D, E) show 3 intensity levels with the large dye-excluded patches being the least intense. This confirms that a difference in dye bleaching efficiency in L_o and L_d phases is not responsible for the observed intensity variations in Fig. 5. The correlated images allow us to draw three conclusions on the restructured bilayer. First, the AFM image shows many small raised features that are similar in size and shape to domains observed prior to enzyme treatment (Fig. 6B, areas outlined in blue). Some of these domains have raised edges, analogous to those assigned to ceramide-rich subdomains in earlier AFM studies [14,25]. The domain heterogeneity is also visible by fluorescence for the larger domains, as indicated by the intensity cross sections shown in Fig. 6E, F. Note that small dark domains with brighter centres are found in other areas, for example area 3 in Fig. 5. Second, the bright fluorescent rings correspond to uniform lower regions in the AFM image, consistent with a disordered DOPC-rich phase. Third, the dark patch (circled in green) in the centre of the bright ring in the fluorescence image has a height intermediate between those of the small ceramide-enriched domains and the lower DOPC-rich regions. This feature shows up clearly in lateral deflection scans (Fig. 6C), and probe **2** suggests that this region is depleted in Chol. The combination of different imaging modes demonstrates that the dark patches in the centre of the bright rings have properties that are different from other regions of the bilayer, consistent with ceramide-enriched platforms formed by enzyme activity. Elsewhere ceramide localizes in small subdomains within and surrounding the original L_o domains. The composition of the two ceramide-enriched regions is likely to be significantly different.

The reorganization of the enzyme-treated bilayers varies for different regions of an individual sample (and from sample to sample) and is attributed to variable numbers of active enzyme molecules in specific regions [25]. The complexity of the enzyme-initiated bilayer restructuring makes it essential to correlate AFM and fluorescence images for the same bilayer area. Correlated AFM and fluorescence

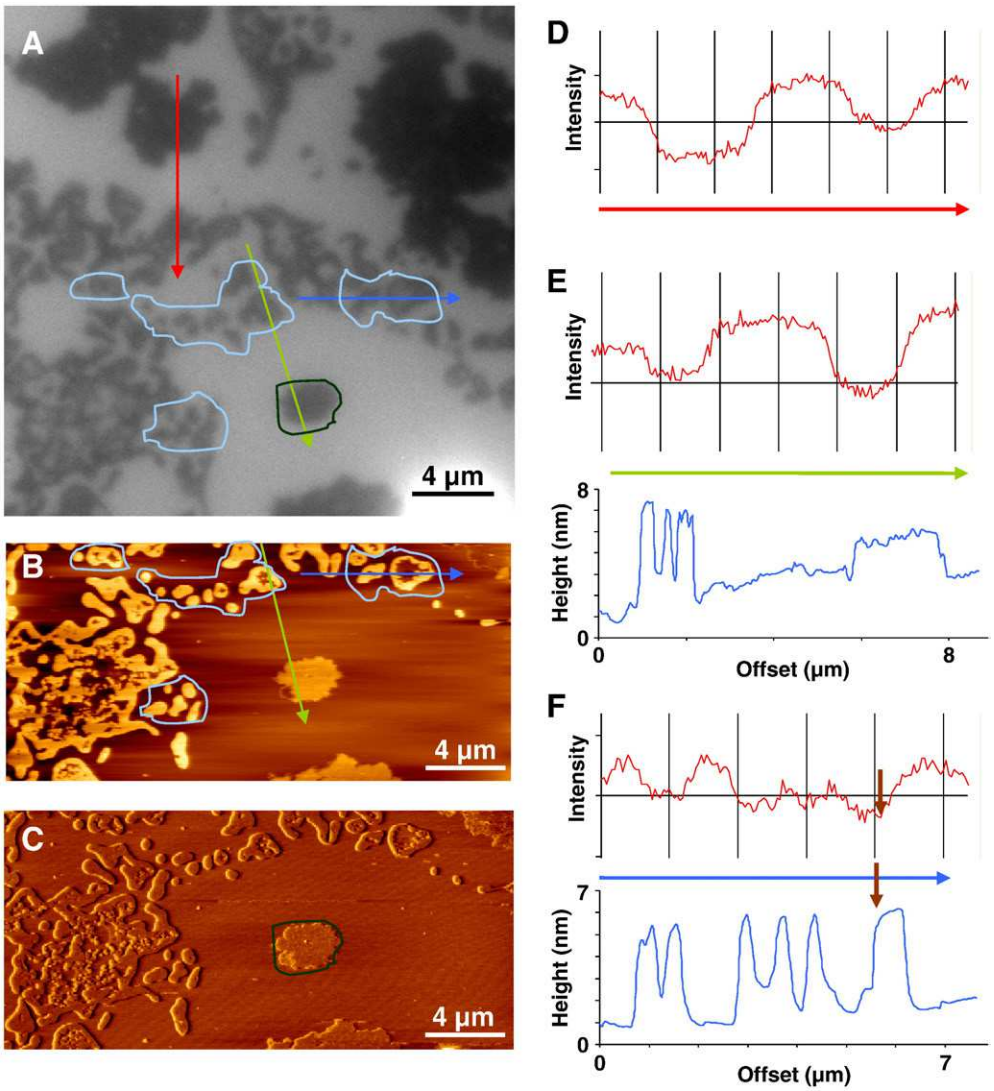

Fig. 6. Correlated fluorescence and AFM images for a DOPC/ESM/Chol (7:9:4 with 0.5 mol% **2**) bilayer that was treated with 0.33 U/ml SMase for 22 min and washed prior to imaging: (A) fluorescence; (B, C) AFM height and lateral deflection images; (D–F) intensity and height cross sections for the lines indicated in images A and B. The large dark patches have lower fluorescence intensity than regions that retain the outlines of the initial domains (D) and show enhanced contrast in lateral deflection (C). Superimposed fluorescence intensity and height cross sections (E) confirm that the domain perimeters are taller and brighter than the dye-excluded patches. Another superposition of intensity and height (F) shows that the domain perimeter (brown arrow) has lower fluorescence than the domain interior.

images for a second SMase-treated bilayer are presented in Fig. S3 to illustrate the range of morphologies produced by enzyme treatment. The results are qualitatively similar to those in Figs. 5 and 6 in that 3 intensity levels are evident in the fluorescence image (Fig. S3A, B) with large dark patches and areas of intermediate intensity that correspond to the initial L_o domains. However, the bright rings of fluid phase are not observed, possibly due to lower enzyme activity. A lateral deflection AFM image (Fig. S1D) shows that the dark areas have high frictional contrast and the smaller domains are heterogeneous with raised edges; both of these effects are attributed to ceramide-rich bilayer regions.

4. Discussion

4.1. NBD-Chol photophysics in lipid bilayers

NBD has strong solvatochromic properties with a quantum yield that decreases with increasing solvent polarity, a property that has been exploited to assess the location and orientation of fluorophore-labeled lipids in membranes [38,40]. In the present study we have observed quantum yields ranging from 0.12 to 0.26 for the various NBD-labeled Chols. By comparison to earlier studies on the solvatochromic properties of n-propylamino-NBD in organic solvents and water-dioxane mixtures, these data indicate a relatively polar environment with dielectric constants between 30 and 40 [38,42]. A wider variation in quantum yields was observed previously for acyl chain labeled NBD-phospholipids that adopt a looping configuration with the NBD group in the relatively polar headgroup region of the bilayer [38].

NBD-Chols **1–3** show only small variations in quantum yield as a function of the linker length in DOPC/Chol and the observed values are similar to those in DOPC as well as to those for NBD-DHPE and the ester-linked NBD-Chol, **5**. This suggests that, in the L_d phase, the polarity of the NBD environment is insensitive to the linker length and the method of fluorophore attachment, consistent with the disordered lipid packing in a fluid bilayer. By contrast, the quantum yields for the DPPC/Chol and ESM/Chol vesicles show larger changes when the linker length is varied from 2 to 6 carbons. Probe **2** with the 4-carbon linker has significantly higher quantum yields, indicative of a less polar environment, than do **1** and **3** which have shorter and longer linkers, respectively. The more polar environment for **3** (with

the 6-carbon linker) is consistent with positioning of the NBD closer to the bilayer interface in a more aqueous environment. It is less obvious why the short two-carbon linker also places the NBD in a more polar environment; one possibility is that the short linker causes significant disruption of headgroup packing, leading to greater water penetration. Interestingly, quantum yields for NBD-DHPE and **5** follow the same trend as **2** in DPPC/Chol and ESM/Chol vesicles, indicating that, despite the change in lipid and method of linker attachment, the fluorophore senses a similar and slightly less polar environment (compared to DOPC) for all three probes. Note that the distance between the Chol oxygen and the dye in ester **5** is almost the same as for probe **2**.

The observation of a less polar environment for **2**, **5** and NBD-DHPE in liquid-ordered vesicles is in contrast to the conclusion that the NBD group in acyl chain labeled lipids is expelled from the bilayer toward the aqueous phase in a gel phase relative to a fluid phase [38]. We attribute this difference to disruptions to lipid packing caused by the looping conformation assumed by the NBD fluorophore for chain labeled phospholipids. Variations in lipid packing and hydration for a Chol-enriched L_o phase, compared to a gel phase, may also play a role [48].

4.2. Fluorescent analogs for modeling free cholesterol

The qualitative partitioning data obtained from fluorescence intensity ratios indicate that the four NBD-Chols show modest preferences for either L_o or L_d phases, depending on the lipid composition and the length and method of attachment of the linker. The estimated partition coefficients show the same general trend in most cases. For the DOPC/DPPC/Chol bilayers, probe **3** shows a significant preference ($K_p = 1.8$) for the L_o domains in DOPC/DPPC/Chol bilayers, whereas probe **1** with the short carbamate linker and ester **5** partition more strongly into the L_d phase. Probe **2** is similar to probe **3** in terms of fluorescence intensity data but after taking changes in probe brightness into account, it actually shows no preference for L_o over L_d phase (K_p of 1). Although the variation in partitioning behavior is relatively modest, the results suggest that the length of the linker and the use of an ester vs carbamate linker do influence probe partitioning. Of the probes that we have examined, a carbamate linker with approximately 13.5 Å between C-3 of cholesterol and C-4 of NBD (probe **3**) gives the highest L_o partitioning.

The data for DOPC/DPPC/Chol mixtures can be compared to recent studies that have used NMR and/or fluorescence to examine phase separation in DOPC, DPPC and Chol mixtures, demonstrating that the L_o phase is strongly enriched in DPPC and moderately enriched in Chol [49,50]. For example, a partition coefficient for Chol of 1.4 was measured for a 1:1 mixture of DOPC/DPPC with 30 mol% Chol at 20 °C [50] and it was concluded that Chol concentrations ranged from 10 to 20 mol% in the L_d phase and 30 to 40% in the L_o phase for 1:1 DOPC/DPPC mixtures with 15 or 30% Chol [49]. These data indicate that **3** (and to a lesser extent **2**) provide reasonably good models for the behavior of native Chol in DOPC/DPPC/Chol mixtures, significantly better than either **1** or **5**. It is evident that relatively small changes to the linker and method of attachment can modulate the partitioning of the NBD-labeled lipids between L_o and L_d phases.

The 3 carbamate-linked NBD-Chols have a reduced preference for the L_o phase for 2:2:1 DOPC/ESM/Chol bilayers, compared to the corresponding DPPC mixtures. Probe **2** does not show a preference for localization in the L_o phase for any of the SM mixtures (including brain SM) that we have examined. The reduced preference for the L_o phase for ESM mixtures compared to DPPC mixtures is consistent with results for several carbocyanine dyes that were shown to partition into the L_d phase for ternary lipid mixtures containing SM but into the L_o phase for DSPC mixtures [28]. By contrast, the ester-linked NBD-Chol, **5**, has a K_p value of 0.4 in both ESM and DPPC ternary lipid mixtures. Interestingly, the Dansyl probe (**4**) has the strongest preference for the L_d phase based on fluorescence intensities in both DPPC and ESM mixtures, consistent with the hypothesis that the less hydrophilic probe may interact more strongly with the bilayer, leading to a preference for the disordered phase.

A recent NMR study of lipid diffusion in DOPC/ESM/Chol mixtures has concluded that Chol partitions to roughly the same extent into both L_o and L_d phases and that the driving force for phase separation in this system is the increasing difficulty of incorporating DOPC into an ordered phase [51]. This observation is in good agreement with the probe partitioning that we observe for **1–3**. However, other studies have shown a strong affinity of cholesterol for ESM or brain SM L_o domains when the unsaturated lipid component is POPC and have concluded that the interaction between Chol and SM is at least as favorable as that between a long chain saturated PC and Chol [52,53]. The lack of quantitative information on the ratio of Chol in L_o and L_d phases for DOPC/ESM/Chol precludes a direct assessment of the ability of the NBD-Chol probes to mimic the behavior of native Chol in the ESM mixture. Nevertheless, the stronger preference of **1–3** for the L_o phase, relative to the ester-linked derivative, is encouraging.

NBD-Chol probes **1–3** have advantages over some of the other fluorescent sterols that have been used to mimic the behavior of free Chol in model membranes [30]. Intrinsically fluorescent sterols, such as cholestatrienol and dehydroergosterol, are generally accepted to be reasonably good models for native Chol. However, they do show differences in NMR order parameters relative to Chol, and their rapid photobleaching and requirement for UV excitation limit their utility for studying biological samples [28,30,32,33]. The two alternate approaches of attaching a fluorophore to either the alkyl side chain or the hydroxyl group of the sterol backbone have met with limited success. As summarized in the introduction, the attachment of polar fluorophores to the alkyl chain generally decreases the affinity for ordered domains and has the added complication of reversing the orientation of Chol so that the fluorophore-labeled tail, rather than the hydroxyl group, is positioned in the polar headgroup region of the bilayer. This limitation can be overcome by conjugation of the relatively non-polar Bodipy to the alkyl chain (so-called Bodipy "free" cholesterol, Bodipy-FChol). The "upright" orientation of this probe in the bilayer is maintained and its partitioning behavior in supported bilayers varies significantly for mixtures containing C_{16}-SM, C_{18}-SM and brain SM, based on qualitative measurements of fluorescence intensities [35]. Measured partition coefficients, $K_p(L_o/L_d)$, of 1.9 and 0.8 for DOPC/egg SM/Chol GUVs and DOPC/C_{18}-SM/Chol supported bilayers confirm the strong dependence on the chain length and heterogeneity of the SM component [13,36]. Interestingly, the three carbamate-linked NBD-Chols studied here show a similar reversal in partitioning for DPPC vs SM mixtures, but not for ESM vs brain SM. Although Bodipy-FChol has the advantage of a higher quantum yield, the use of hydroxyl-labeled Chols may be advantageous in cases where it is preferable to avoid introducing a dye in the bilayer interior.

Although several Chol analogs with doxyl spin labels attached to the hydroxyl group adequately model the behavior of natural Chol [32], attaching Bodipy to this position via an ester linker produces a probe that partition strongly into Lo domains. For example, a Bodipy-Chol ester with the dye attached via a C_{12} alkyl chain has K_p (L_o/L_d) = 0.16 in DOPC/SM/Chol supported bilayers as measured by FCS) [37]. By contrast, the carbamate-linked NBD-Chols that we have synthesized show significantly stronger preferences for the L_o phase in both DPPC and ESM ternary lipid mixtures. This confirms our hypothesis that the partitioning of the Bodipy-Chol ester is dominated by the propensity for Bodipy to insert into the alkyl chain region of the membrane, disrupting lipid packing. The carbamate-linked NBD probes show close to 2-fold higher partitioning into L_o domains than does the commercial ester-linked NBD probe, **5**. Like hydroxyl groups, carbamates can act as both hydrogen bond donors and acceptors, and the presence of this functional group may allow these probes to behave more like free Chol in model membranes. The Dansyl analog, **4**, has a considerably

lower I_{Lo}/I_{Ld} that any of the NBD-Chol analogs in both ESM and DPPC mixtures. This is likely due to incorporation of the less polar Dansyl into the hydrophobic region of the bilayer, similar to Bodipy. Although effects of changes in probe brightness were not measured for **4**, literature data on solvatochromic properties of Dansyl fluorophores suggest that variations in fluorescence efficiency will be comparable to those for NBD [54].

The ability of probe **2** to mimic the well-known exclusion of Chol from ceramide-rich membrane domains was also examined. The displacement of **2** from ceramide domains was confirmed by correlated AFM and fluorescence imaging. A number of methods have provided convincing evidence for the expulsion of Chol by ceramide [12,16–19] and Bodipy-FChol has recently provided the first direct optical visualization of this phenomenon in DOPC/SM/Chol/Cer supported bilayers [13]. However, unlike Bodipy-FChol, NBD-Chol **2** has the advantage of allowing simultaneous visualization of all three coexisting phases (ceramide-rich, L_o and L_d) produced by direct incorporation of ceramide in DOPC/ESM/Chol bilayers with a single probe. Together, our work plus the previous study using Bodipy-FChol, suggest that designing a probe to reproduce the exclusion of Chol from ceramide-rich domains is more straightforward than designing one to mimic the more subtle interactions of Chol with PC or SM in L_o domains.

4.3. Probing cholesterol redistribution during in situ generation of ceramide in phase separated bilayers

NBD-Chol **2** was used to follow changes in bilayer morphology and Chol redistribution during enzymatic generation of ceramide in DOPC/ESM/Chol bilayers. Although the initial fluorescence intensities for probe **2** are similar in L_o domains and the surrounding L_d phase, the contrast is adequate to visualize the domains and to show that the overall bilayer restructuring induced by SMase is analogous to that observed in our earlier studies using Texas Red-DHPE, which has a strong preference for the L_d phase [24,25]. The use of NBD-Chol **2** has two important advantages, as discussed below: (1) it allows visualization of the dynamic reorganization of Chol during enzyme activity and (2) it provides information on the composition of various regions of the restructured bilayer.

Bilayers that initially have only two levels of fluorescence intensity, corresponding to L_d and L_o phases identified by AFM, evolve to show greater heterogeneity upon exposure to SMase. The L_o domains show progressively lower fluorescence intensity, with concomitant formation of bright rings of fluid phase around large dye-excluded patches (Figs. 6 and S3). This provides the first direct visualization of the dynamic displacement of Chol from liquid-ordered domains in response to *in situ* enzymatic ceramide production. Changes in domain structure and evolution from a mixture of L_o and L_d phases to a gel and liquid phase have been reported after enzymatic generation of ceramide in GUVs of ternary lipid mixtures [26]. A related fluorescence microscopy study has provided evidence for pore formation and vesicle collapse for SMase-treated GUVs [23]. Of particular interest, Silva et al. have examined enzymatic hydrolysis of SM in PSM/POPC/Chol vesicles, a lipid mixture for which a detailed phase diagram is available [27]. This work demonstrated that the physical properties of the membrane strongly modulate SMase activity with phase separated (L_o/L_d) mixtures showing higher activity. The effects of ceramide were dependent on the Chol concentration, leading to the hypothesis that Chol in particular, and lipid rafts in general, function as modulators of SMase in cells [27]. The development of specific probes to track Chol will facilitate a better understanding of the complex bilayer changes that occur after enzymatic ceramide generation, as illustrated here for one lipid mixture.

The domain heterogeneity produced by ceramide generation and concomitant Chol expulsion are clearly visualized by AFM which shows raised ceramide-enriched regions around many of the initial L_o domains. These ceramide "fences" are believed to form at the perimeter of the SM-rich domains because the interface between the two phases is disordered, facilitating access of the enzyme to its substrate [14,55,56]. Although the domain heterogeneity is typically below the resolution limit of fluorescence microscopy, there are some larger domains that do show two levels of fluorescence after enzyme treatment (Fig. 6), with the darker domain perimeter corresponding to raised domain edges in the AFM. The loss of **2** from the ceramide-enriched regions in enzyme-treated bilayers is consistent with the exclusion of probe **2** from ceramide-enriched domains when ceramide is directly incorporated in DOPC/ESM/Chol bilayers.

In addition to observing the dynamic reorganization of Chol, probe **2** provides insight on the composition of the large dye-excluded patches that form during enzyme activity. In earlier studies using AFM and fluorescence imaging with Texas Red-DHPE as a probe, it was not possible to assign the composition of these new membrane regions. Although we initially hypothesized that the dye-excluded patches were enriched in Chol, AFM showed that they had high lateral adhesion, more consistent with ceramide-enriched regions [14,25]. The use of probe **2** demonstrates that the large dye-excluded patches that form during enzyme activity exclude Chol, leading to the conclusion that they are ceramide-enriched membrane regions. The SMase-induced coalescence of small raft domains to form larger ceramide platforms has been postulated to provide a mechanism for modulating signaling processes [4,5]. Nevertheless, most of the available evidence suggests that ceramide forms small gel phase domains that are unlikely to localize membrane proteins. The recent study of ceramide-induced membrane alterations by Silva et al. has suggested that platforms may be Chol-enriched SM-depleted L_d domains [27]. Our work indicates that large ceramide-enriched regions can form, at least in supported bilayers. Additional studies of the properties of these ceramide-enriched regions and their ability to include signaling molecules will be necessary to assess their relevance to the ceramide-enriched platforms that are hypothesized to form in cells.

5. Conclusions

A series of Chol probes with NBD attached to the 3-hydroxyl position via carbamate linkers with variable lengths has been synthesized based on rational design principles. The photophysical properties of the probes have been characterized and their partitioning in phase separated supported bilayers estimated based on L_o/L_d fluorescence intensity ratios. The carbamate-linked NBD-Chols show a stronger preference for partitioning into L_o domains than does a structurally similar probe with an ester linkage, **5**, illustrating the importance of careful optimization of probe and linker to provide the best mimic of free Chol. Comparison of the partitioning of NBD probes to available literature data for Chol indicates that the probes reproduce well the relatively modest enrichment of Chol in L_o vs L_d domains for DOPC/DPPC/Chol mixtures as well as the ceramide-induced displacement of Chol. Probe **2** was used to follow the dynamic redistribution of Chol in phase separated membrane in response to *in situ* ceramide generation. This provides the first direct optical visualization of Chol redistribution during enzymatic ceramide generation and allows the assignment of new bilayer regions that exclude dye and have high lateral adhesion to ceramide-rich regions. Overall this study illustrates the feasibility of the rational design of fluorophore-labeled lipids to track specific bilayer components and the utility of a correlated AFM-fluorescence imaging approach for probing complex bilayer morphology.

Acknowledgements

This work was supported by Natural Science and Engineering Research Council operating grants to WWO and LJJ.

Appendix A. Supplementary data

Supplementary data associated with this article can be found, in the online version, at doi:10.1016/j.bbamem.2009.12.005.

References

[1] K. Simons, W.L. Vaz, Model systems, lipid rafts and cell membranes, Annu. Rev. Biophys. Biomol. Struct. 33 (2004) 269–295.
[2] K. Simons, E. Ikonen, Functional rafts in cell membranes, Nature 387 (1997) 569–572.
[3] S. Mayor, M. Rao, Rafts: scale-dependent, active lipid organization at the cell surface, Traffic 5 (2004) 231–240.
[4] A.E. Cremesti, F.M. Goni, R. Kolesnick, Role of sphingomyelinase and ceramide in modulating rafts: do biophysical properties determine biologic outcome? FEBS Lett. 531 (2002) 47–53.
[5] C.R. Bollinger, V. Teichgraber, E. Gulbins, Ceramide-enriched membrane domains, Biochim. Biophys. Acta 1746 (2005) 284–294.
[6] R.N. Kolesnick, F.M. Goni, A. Alonso, Compartmentalization of ceramide signaling: physical foundations and biological effects, J. Cell Physiol. 184 (2000) 285–300.
[7] Y.A. Hannun, C. Luberto, K.M. Argraves, Enzymes of sphingolipid metabolism: from modular to integrative signaling, Biochem. 40 (2001) 4893–4903.
[8] F.M. Goni, A. Alonso, Effects of ceramide and other simple sphingolipids on membrane lateral structure, Biochim. Biophys. Acta 1788 (2009) 169–177.
[9] B.C. Lagerholm, G.E. Weinreb, K. Jacobson, N.L. Thompson, Detecting microdomains in intact cell membranes, Annu. Rev. Phys. Chem. 56 (2005) 309–336.
[10] E. London, How principles of domain formation in model membranes may explain ambiguities concerning lipid raft formation in cells, Biochim. Biophys. Acta 1746 (2005) 203–220.
[11] S.L. Veatch, S.L. Keller, Seeing spots: complex phase behavior in simple membranes, Biochim. Biophys. Acta 1746 (2005) 172–185.
[12] S. Chiantia, N. Kahya, H. Ries, P. Schwille, Effects of ceramide on liquid-ordered domains investigated by simultaneous AFM and FCS, Biophys. J. 90 (2006) 4500–4508.
[13] S. Chiantia, J. Ries, G. Chwastek, D. Carrer, Z. Li, R. Bittman, P. Schwille, Role of ceramide in membrane protein organization investigated by combined AFM and FCS, Biochim. Biophys. Acta 1778 (2008) 1356–1364.
[14] Ira, L.J. Johnston, Ceramide promotes restructuring of model raft membranes, Langmuir 22 (2006) 11284–11289.
[15] L. Silva, R.F.M. de Almeida, A. Federov, A.P.A. Matos, M. Prieto, Ceramide-platform formation and induced biophysical changes in a fluid phospholipid membrane, Mol. Membr. Biol. 23 (2006) 137–148.
[16] L.C. Silva, R.F.M. de Almeida, B.M. Castro, A. Fedorov, M. Prieto, Ceramide-domain formation and collapse in lipid rafts: membrane reorganization by an apoptotic lipid, Biophys. J. 92 (2007) 502–516.
[17] Megha, P. Sawatzki, T. Kolter, R. Bittman, E. London, Effect of ceramide N-acyl chain and polar headgroup structure on the properties of ordered lipid domains (lipid rafts), Biochim. Biophys. Acta 1768 (2007) 2205–2212.
[18] Megha, E. London, Ceramide selectively displaces cholesterol from ordered lipid domains (rafts): implications for lipid raft structure and function, J. Biol. Chem. 279 (2004) 9997–10004.
[19] M.R. Ali, K.H. Cheng, J. Huang, Ceramide drives cholesterol out of the ordered lipid bilayer phase into the crystal phase in 1-palmitoyl-2-oleoyl-*sn*-glycero-3-phosphocholine/cholesterol/ceramide ternary mixtures, Biochem. 45 (2006) 12629–12638.
[20] J. Sot, M. Ibarguren, J.V. Busto, L.-R. Montes, F.M. Goni, A. Alonso, Cholesterol displacement by ceramide in sphingomyelin-containing liquid-ordered domains, and in generation of gel regions in giant lipidic vesicles, FEBS Lett. 582 (2008) 3230–3236.
[21] T.A. Nurminen, J.M. Holopainen, H. Zhao, P.K. Kinnunen, Observation of topical catalysis by sphingomyelinase coupled to microspheres, J. Am. Chem. Soc. 124 (2002) 12129–12134.
[22] D.C. Carrer, B. Maggio, Phase behavior and molecular interactions in mixtures of ceramide with dipalmitoylphosphatidylcholine, J. Lipid Res. 40 (1999) 1978–1989.
[23] I. Lopez-Mentero, M. Velez, P.F. Devaux, Surface tension induced by sphingomyelin to ceramide conversion in lipid membranes, Biochim. Biophys. Acta 1768 (2007) 553–561.
[24] Ira, L.J. Johnston, Sphingomyelinase generation of ceramide promotes clustering of nanoscale domains in supported bilayer membranes, Biochim. Biophys. Acta 1778 (2008) 185–197.
[25] [25] Ira, S. Zou, D. Carter Ramirez, S. Vanderlip, W. Ogilvie, Z. Jakubek and L.J. Johnston, Enzymatic generation of ceramide induces membrane restructuring: correlated AFM and fluorescence imaging of supported bilayers, J. Struct. Biol. 168 (2009) 78–89.
[26] Y. Taniguchi, T. Ohba, H. Miyata, K. Ohki, Rapid phase change of lipid microdomains in giant vesicles induced by conversion of sphingomyelin to ceramide, Biochim. Biophys. Acta 1758 (2006) 145–153.
[27] L.C. Silva, A.H. Futerman, M. Prieto, Lipid raft composition modulates sphingomyelinase activity and ceramide-induced membrane physical alterations, Biophys. J. 96 (2009) 3210–3222.
[28] T. Baumgart, G. Hunt, E.R. Farkas, W.W. Webb, G.W. Feigenson, Fluorescence probe partitioning between Lo/Ld phases in lipid membranes, Biochim. Biophys. Acta 1768 (2007) 2182–2194.
[29] P. Sengupta, A. Hammond, D. Holowka, B. Baird, Structural determinants for partitioning of lipids and proteins between coexisting fluid phases in giant plasma membrane vesicles, Biochim. Biophys. Acta 1778 (2008) 20–32.
[30] D. Wustner, Fluorescent sterols as tools in membrane biophysics and cell biology, Chem. Phys. Lipids 146 (2007) 1–25.
[31] Y.J.E. Bjorkqvist, T.K.M. Nyholm, J.P. Slotte, B. Ramstedt, Domain formation and stability in complex lipid bilayers as reported by cholestatrienol, Biophys. J. 88 (2005) 4054–4063.
[32] H.A. Scheidt, P. Muller, A. Herrmann, D. Huster, The potential of fluorescent and spin-labeled steroid analogs to mimic natural cholesterol, J. Biol. Chem. 278 (2003) 45563–45569.
[33] D. Wustner, Improved visualization and quantitative analysis of fluorescent membrane sterol in polarized hepatic cells, J. Micros. 220 (2005) 47–64.
[34] Z. Li, E. Mintzer, R. Bittman, First synthesis of free cholesterol-BODIPY conjugates, J. Org. Chem. 71 (2006) 1718–1721.
[35] J.E. Shaw, R.F. Epand, R.M. Epand, Z. Li, R. Bittman, C.M. Yip, Correlated fluorescence-atomic force microscopy of membrane domains: structure of fluorescence probes determines lipid localization, Biophys. J. 90 (2006) 2170–2178.
[36] F.S. Ariola, Z. Li, C. Cornejo, R. Bittman, A.A. Heikal, Membrane fluidity and lipid order in ternary giant unilamellar vesicles using a new Bodipy-cholesterol derivative, Biophys. J. 96 (2009) 2696–2708.
[37] S. Chiantia, J. Ries, N. Kahya, P. Schwille, Combined AFM and two-focus SFCS study of raft-exhibiting model membranes, Chem. Phys.Chem. 7 (2006) 2409–2418.
[38] S. Mazeres, V. Schram, J.-F. Tocanne, A. Lopez, 7-Nitrobenz-2-oxa-1, 3-diazole-4-yl-labeled phospholipids in lipid membranes: differences in fluorescence behavior, Biophys. J. 71 (1996) 327–335.
[39] W.J. Galush, J.A. Nye, J.T. Groves, Quantitative fluorescence microscopy using supported lipid bilayer standards, Biophys. J. 95 (2008) 2512–2519.
[40] A. Chattopadhyay, Chemistry and biology of N-(7-nitrobenz-2-oxa-1, 3-diazol-4-yl)-labeled lipids: fluorescent probes of biological and model membranes, Chem. Phys. Lipids 53 (1990) 1–15.
[41] V. Wiegand, T.-Y. Chang, J.F. Strauss, F. Fahrenholz, G. Gimpl, Transport of plasma membrane-derived cholesterol and the function of Niemann–Pick C1 protein, FASEB J. 17 (2003) 782–784.
[42] S. Fery-Forgues, J.-P. Fayet, A. Lopez, Drastic changes in the fluorescence properties of NBD probes with the polarity of the medium: involvement of a TICT state? J. Photochem. Photobiol. A: Chem. 70 (1993) 229–243.
[43] S.L. Veatch, S.L. Keller, Separation of liquid phases in giant vesicles of ternary mixtures of phospholipids and cholesterol, Biophys. J. 85 (2003) 3074–3083.
[44] S.L. Veatch, S.L. Keller, Miscibility phase diagrams of giant vesicles containing sphingomyelin, Phys. Rev. Lett. 94 (2005) 148101.
[45] J.E. Shaw, J. Oreopoulos, D. Wong, J.C.Y. Hsu, C.M. Yip, Coupling evanescent-wave fluorescence imaging and spectroscopy with scanning probe microscopy: challenges and insights from TIRF-AFM, Surf. Interface Anal. 38 (2006) 1459–1471.
[46] V. Coste, N. Puff, D. Lockau, P.J. Quinn, M.I. Angelova, Raft-like domain formation in large unilamellar vesicles probes by the fluorescent phospholipid analogue, C12NBD-PC, Biochem. Biophys. Acta 1758 (2006) 460–467.
[47] R.M.A. Sullan, J.K. Li, S. Zou, Direct correlation of structures and nanomechanical properties of multicomponent lipid bilayers, Langmuir 25 (2009) 7471–7477.
[48] A.P. Demchenko, Y. Mély, G. Duportail, A.S. Klymchenko, Monitoring biophysical properties of lipid membranes by environment-sensitive fluorescent probes, Biophys. J. 96 (2009) 3461–3470.
[49] G. Oradd, P.W. Westerman, G. Lindblom, Lateral diffusion coefficients of separate lipid species in a ternary raft-forming bilayer: a pfg-NMR multinuclear study, Biophys. J. 89 (2005) 315–320.
[50] S.L. Veatch, I.V. Polozov, K. Gawrisch, S.L. Keller, Liquid domains in vesicles investigated by NMR and fluorescence microscopy, Biophys. J. 86 (2004) 2910–2922.
[51] G. Lindblom, G. Oradd, A. Filipov, Lipid lateral diffusion in bilayers with phopphatidylcholine, spingomylein and cholesterol. An NMR study of dynamics and lateral phase separation, Chem. Phys. Lipids 141 (2006) 179–184.
[52] M.L. Frazier, J.R. Wright, A. Pokorny, P.F.F. Almeida, Investigation of domain formation in sphingomyelin/cholesterol/POPC mixtures by fluorescence resonance energy transfer and Monte Carlo simulations, Biophys. J. 92 (2007) 2422–2433.
[53] A. Tsamaloukas, H. Szadkowska, H. Heerklotz, Thermodynamic comparison of the interactions of cholesterol with unsaturated phospholipid and sphingomyelins, Biophys. J. 90 (2006) 4479–4487.
[54] Y.-H. Li, L.-M. Chan, L. Tyer, R.T. Moody, C.M. Himel, D.M. Hercules, Study of solvent effects on the fluorescence of 1-(Dimethylamino)-5-naphthalenesulfonic acid and related compounds, J. Am. Chem. Soc. 97 (1975) 3118–3126.
[55] H.X. You, L. Yu, X. Qi, Phospholipid membrane restructuring induced by saposin C: a topographic study using atomic force microscopy, FEBS Lett. 503 (2001) 97–102.
[56] M. Grandbois, H. Clausen-Schaumann, H. Gaub, Atomic force microscope imaging of phospholipid bilayer degradation by phospholipase A_2, Biophys. J. 74 (1998) 2398–2404.